01 May 1989

Spectroscopy of the $6p_{3/2}np$ States of Barium

J. Greg Story
Missouri University of Science and Technology, story@mst.edu

E. G. Yap

William E. Cooke

Recommended Citation

J. G. Story et al., "Spectroscopy of the $6p_{3/2}np$ States of Barium," *Physical Review A*, vol. 39, no. 10, pp. 5127-5131, American Physical Society (APS), May 1989.
The definitive version is available at https://doi.org/10.1103/PhysRevA.39.5127

PHYSICAL REVIEW A VOLUME 39, NUMBER 10 MAY 15, 1989

Spectroscopy of the $6p_{3/2}np$ states of barium

J. G. Story, E. G. Yap, and W. E. Cooke
Department of Physics, University of Southern California, Los Angeles, California 90089-0484
(Received 22 December 1988)

The $6p_{3/2}np$ states of barium have been observed for n values between 14 and 21. The energies, linewidths, and transition strengths have been measured and characterized in terms of one- and two-electron interactions, using a single-configuration approximation.

INTRODUCTION

Beginning in the mid 1970s, developments in dye laser spectroscopy made it possible to accumulate large quantities of spectroscopic data about the energy levels of the two-electron-like alkaline-earth atoms.[1] The quantity and quality of the data mandated a new analysis tool which could be used to reduce this data to a relatively small number of parameters. Near simultaneous developments in multichannel quantum-defect theory (MQDT) provided the ideal analysis tool since it treated configuration mixing among entire Rydberg series in a self-consistent manner.[2–4] The thrust of this work was usually that *all* states of the same total angular momentum J and of the same parity must be treated simultaneously, to account for the small, but easily observable, deviations of the bound states from the positions predicted by a crude quantum-defect analysis. This was a significant departure from the more traditional spectroscopic analyses which used *splittings* between multiplets of the same configuration, but different J values.

During the 1980s, a new technique for studying doubly excited states of two-electron atoms was developed, and this resulted in a considerable amount of new spectroscopic information about the autoionizing spectra of these atoms.[5,6] But these states seldom showed much evidence of configuration mixing, as their energies were usually well characterized by a single quantum defect. Nevertheless, considerable effort has been devoted to MQDT analyses of these states to show that this method can be used and will accurately reproduce some of the more surprising aspects of the spectra. However, what has not usually been done with this data, is to analyze it in terms of a single configuration with splittings between the various J states produced by one- and two-electron interactions.

Here, we have observed and analyzed five components of the $6p_{3/2}np$ multiplet for $n=14$ to 21 in barium. Our excitation and detection techniques are similar to those used elsewhere, but our analysis attempts to explain the splittings within this multiplet, rather than the coupling of any one of these states to other configurations of the same parity and J. We find that these splittings can be explained in terms of (1) the two-electron, direct and exchange, monopole and quadrupole interactions; and (2) the one-electron spin-orbit interaction. As a consistency check on this analysis, we have also compared predictions and measurements for excitation strengths and autoionization rates to the $6p_{1/2}\epsilon p$ continuum. As a final check, we have found reasonable agreement with a calculation of these interactions based on a single-configuration, frozen-core, Hartree-Fock method that uses a model potential for the Ba^{2+} core.

THEORY

The $6pnp$ states of barium might seem to be poor candidates for a single-configuration analysis, at first glance. The "core" $6p$ electron is optically active, having strong dipole transitions in the 400- to 650-nm range. However, the "Rydberg" np electron has its transition strength well localized in the far ir range, and this frequency mismatch results in a relatively pure $6pnp$ series. In fact, the Rydberg spacing for states of $n \geq 12$ is small even when compared to the $Ba^{+}(6p_j)$ fine-structure splitting (1691 cm^{-1}), so that the $6p_{3/2}np$ states form a well-defined single-configuration multiplet by themselves. Moreover, the $6pnp$ states of barium lie well above the ionization limit, and autoionize on a time scale of 10 to 100 classical orbit periods. This, of course, represents a considerable configuration mixing; however, it does not cause significant energy shifts, but only broadens the states, as long as the autoionization interaction is not strongly energy dependent. Such interactions almost never change on an energy scale comparable to a few Rydberg states' spacings. Usually, this broadening will make it more difficult to measure a state's energy to a high accuracy, but this also makes breakdowns of the single-configuration approximation less apparent.

A $6p_{3/2}np$ multiplet consists of six states with J values ranging from 0 to 3. There are two states each with J values of 1 and 2. Our excitation scheme uses two photons to excite these states, so only the $J=3$ state is inaccessible. In a single-configuration model, the energies of these states are determined by the electrostatic interaction between the two electrons, and the spin-orbit interaction of the outer, Rydberg electron. The electrostatic interaction can be written in terms of the Slater integrals between the two electrons' wave functions[7]

$$F^k(nl;n'l')=e^2\int \frac{r_<^k}{r_>^{k+1}} R_{nl}^2(r_1)R_{n'l'}^2(r_2)r_1^2dr_1r_2^2dr_2 \ , \tag{1}$$

$$G^k(nl;n'l')=e^2\int \frac{r_<^k}{r_>^{k+1}}R_{nl}(r_1)R_{n'l'}(r_1)R_{nl}(r_2) \times R_{n'l'}(r_2)r_1^2dr_1r_2^2dr_2 \ . \quad (2)$$

For the $6pnp$ configuration, only the F^0, G^0, F^2, and G^2 terms can contribute, since two p wave functions can only be coupled together by monopole or quadrupole interactions. The F^0, which represents the shielding of the core by the inner electron, will produce the same contribution to all states of the multiplet, and consequently will not give rise to a splitting. We will ignore it for our purposes. The remaining exchange monopole term (G^0), and direct and exchange quadrupole terms (F^2 and G^2, respectively) are diagonal in LS coupling and give rise to energy shifts as follows:[7]

$$\Delta E(^{1,3}S)=\tfrac{2}{5}F^2\pm(G^0+\tfrac{2}{5}G^2) \ , \quad (3)$$

$$\Delta E(^{1,3}P)=-\tfrac{1}{5}F^2\mp(G^0-\tfrac{1}{5}G^2) \ , \quad (4)$$

$$\Delta E(^{1,3}D)=\tfrac{1}{25}F^2\pm(G^0+\tfrac{1}{25}G^2) \ , \quad (5)$$

where the upper sign corresponds to the singlet term and the lower sign corresponds to the triplet term. The coefficients arise from the angular integrations.

Of course, the states are not actually LS coupled, due to the spin-orbit couplings of each electron. This coupling is most important for the core $6p$ electron; however, it is not negligible even for the Rydberg np electron. To account for these effects, one can transform the LS-coupled states to jj-coupled states via unitary transformations given by the $9j$ symbols.[7] This transformation will also transform the energies of Eq. (3) through Eq. (5) into an energy matrix with both diagonal and off-diagonal matrix elements. The one-electron spin-orbit effects can then be easily introduced as diagonal terms for the various $6p_jnp_{j'}$ configurations, as follows:

$$\Delta E(6p_jn_{j'})=(1127\text{cm}^{-1})(j-1)(j+\tfrac{1}{2})+\xi(j'-1)(j'+\tfrac{1}{2}) , \quad (6)$$

where 1127 cm^{-1} and ξ are $\frac{2}{3}$ of the $6p$ core electron and of the np Rydberg electron fine-structure splittings, respectively.

The total energy matrix for each value of J separates into two submatrices, since the $6p$ fine-structure splitting is large compared to all the other interactions. Within each submatrix, the energies and state composition can readily be determined by diagonalizing the submatrix to obtain its eigenvalues and eigenvectors. For two J values, $J=0$ and $J=3$, this represents no effort at all, since they are both 1×1 matrices. The diagonalization of the $J=1$ and $J=2$ submatrices depends on the specific values of F^2, G^0, G^2 and ξ. The elements coupling the two submatrices represent autoionization of $6p_{3/2}np$ states into $6p_{1/2}\epsilon p$ continua at a rate of

$$\Gamma=2\pi|V|^2n^{*3} \ , \quad (7)$$

where Γ is the autoionization rate into the specific $6p\epsilon p$ continuum, V is the matrix element from above, and n^{*3} changes the normalization of the bound $6p_{1/2}np$ state into that of a continuum $6p_{1/2}\epsilon p$ state, normalized per unit energy.[8] It is an excellent approximation to use a rescaled bound-state wave function as a continuum wave function, since the continuum electron has a very low energy.

EXPERIMENT

The measurements consisted of determining the $6p_{3/2}np$ states' energies, their linewidths, their relative excitation strengths using two different combinations of excitation laser polarizations, and finally, their relative efficiencies for producing excited $Ba^+(6p_{1/2})$ ions after autoionization. All of the measurements were performed using the Isolated Core Excitation technique, in which one electron is first excited to a bound, Rydberg state, and then the remaining core electron is excited, while the Rydberg electron remains a spectator.[5,6]

Figure 1 illustrates this process for exciting a $6p_{3/2}np$ state of barium. First, a uv photon near 240 nm from a doubled dye laser excites the $6s^2\rightarrow6snp\ ^1P_1$ transition in atomic barium. Armstrong *et al.*[9] have reported an extensive listing of the required wavelengths for these transitions. Then, a second laser, near 455 nm excites the doubly excited state, $6s6p\ ^1P_1\rightarrow6p_{3/2}np$ by driving the core transition. Since the bound Rydberg state is nearly a pure $^1P_1$ configuration, the excitation is almost entirely to the singlet character of the final $6p_{3/2}np$ state. The two linearly polarized lasers can be combined with either parallel or perpendicular relative polarizations, to excite either the $^1S_0$ and $^1D_2$ character, or the $^1P_1$ and $^1D_2$ character of the $6p_{3/2}np$ states.

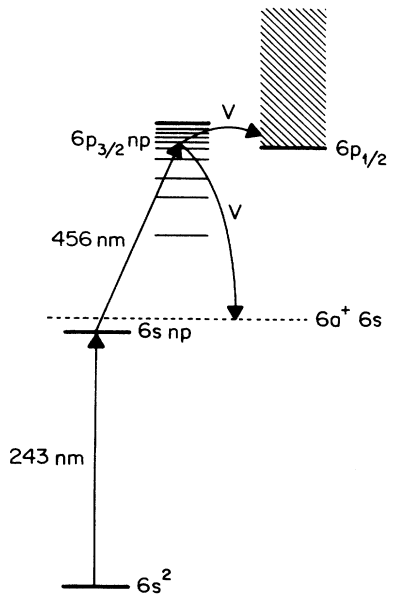

FIG. 1. Energy-level diagram for exciting the $6p_{3/2}np$ states of barium. Autoionization leads to either excited $6p_{1/2}$ ions which then fluoresce, or to ground-state ions. (The $5d$ ionic state has been eliminated for clarity, since it does not fluoresce.)

The lasers are pumped by the third harmonic of two independently timed Nd:YAG (where YAG is yttrium aluminum garnet) lasers. Both pump lasers have 10-ns-pulse widths, and the resulting dye lasers typically have powers of 0.5–2 mJ, linewidths of 0.6 cm^{-1}, and pulse lengths of 2 ns. The first dye laser is doubled using an angle-tuned β-BBO (beta barium borate) crystal. The two lasers are combined colinearly by a dichroic beamsplitter, and cross one of two effusive atomic beams at a right angle.

In one apparatus, the lasers cross the atomic beam in a region between two parallel plates. These plates were used to accelerate the resulting ions out of the interaction region, and into a microchannel plate detector. In the other apparatus, a lens system collects any fluorescence from the atoms or residual ions, and focuses it onto the entrance slits of an $\frac{1}{8}$-m monochromator. This monochromator was set to detect only fluorescence from $6p_{1/2}$ ions resulting from autoionization. In either case, a laboratory microcomputer scanned the second core laser, and recorded the signal after it was accumulated by a boxcar integrator.

It was especially important to maintain a low intensity of the second dye laser during these excitations. The core transitions are very strong, so that it only takes 1 $\mu J/cm^2$ to saturate the transition to a 1 cm^{-1} wide autoionizing state. Saturation of the transition at line center results in anomalously broad lines with constant amplitudes.[10] In order to obtain reliable measurements of the states' linewidths and their transition strengths, we repeatedly lowered the core laser intensity until the signal amplitude was linear in laser power, but the linewidth was independent of it.

RESULTS AND DISCUSSION

The excitation spectra provided straightforward values for the energies and linewidths for four of the five $J=0$, 1, and 2 states of the $6p_{3/2}np$ multiplet. One $J=1$ state was typically small and hidden by a larger, nearby $J=2$ state. The $J=3$ state was not excited, since only two photons were used. Figure 2 shows the quantum-defects of the four measured states as a function of n. They lie along a straight line, as expected for unperturbed configurations. The linewidths of the states also follow an unperturbed n^{*-3} scaling, although many of the higher states' linewidths were obscured by the 0.6 cm^{-1} laser linewidth. This strongly suggests the absence of any appreciable perturbation due to a configuration with a different core state (such as a $7s^2$ perturber). The entire multiplet has a spread in quantum defects of approximately 0.3, so that perturbation theory should be adequate for the splitting within one $6p_{3/2}np$ configuration. The excitation spectra showed no sign of admixture of other core-degenerate configurations, such as the $6p_{3/2}nf$.

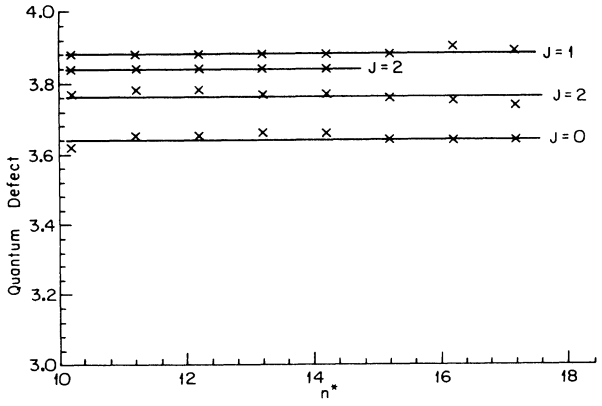

FIG. 2. Quantum defects for the $6p_{3/2}np$ states of barium. The straight lines show that there is little effect of perturbing configurations.

Similar data taken for the $6p_{1/2}np$ states showed serious deviations from constant quantum defects and n^{*-3} scaling of the linewidths. However, this is to be expected, since the same interactions that cause splittings in the $6p_{3/2}np$ multiplet will cause configuration mixing between a $6p_{1/2}np$ state and a $6p_{3/2}n'p$ perturber resulting in energy-dependent shifts. The complementary effect on the $6p_{3/2}np$ states, with $n \geq 12$, is an energy independent increase in autoionization into the $6p_{1/2}\epsilon p$ continuum. Efforts to treat the entire spectrum in a self-consistent manner are currently under way.

Typical data showing the total excitation spectrum and the fluorescence from the residual ions is shown in Fig. 3. Since this is a relatively low state ($n=15$), four states are readily visible, and the remaining $J=1$ state is just discernable as a small feature on the high-energy side of the major $J=2$ peak. Figures 3(a) and 3(b) show excitation spectra where all ions produced by autoionization are collected. Figure 3(a) shows an excitation spectrum taken with parallel polarized lasers, so only the two $J=2$ states and the broad $J=0$ state should be excited. A $J=1$ peak is visible at 21 915 cm^{-1}, but we attribute it to a small admixture of circularly polarized light in the core laser. Figure 3(b) shows a similar excitation spectrum taken with perpendicularly polarized lasers, so that only $J=1$ and $J=2$ states can be excited. Figures 3(c) and 3(d) show spectra obtained by detecting fluorescence emitted by the $Ba^+(6p_{1/2})$ ions after autoionization. Notice how this enhances the $J=0$ and $J=1$ resonances.

To reduce the spectral information to the electron interactions of Eqs. (1) and (2), we analyzed the $6p_{3/2}15p$ states in detail. Specifically, we adjusted the four parameters F^2, G^0, G^2, and ξ to obtain the best possible fit for the energy of each resonance, relative to the large $J=2$

TABLE I. Two-electron Slater integrals and the Rydberg fine-structure interaction as determined from the $6p_{1/2}15p$ spectrum and from the two-electron model wave functions.

Interaction	Measured (cm^{-1})	Calculated (cm^{-1})
F^2	60±5	66
G^0	6±1	10
G^2	10±4	16
ξ	5±2	4

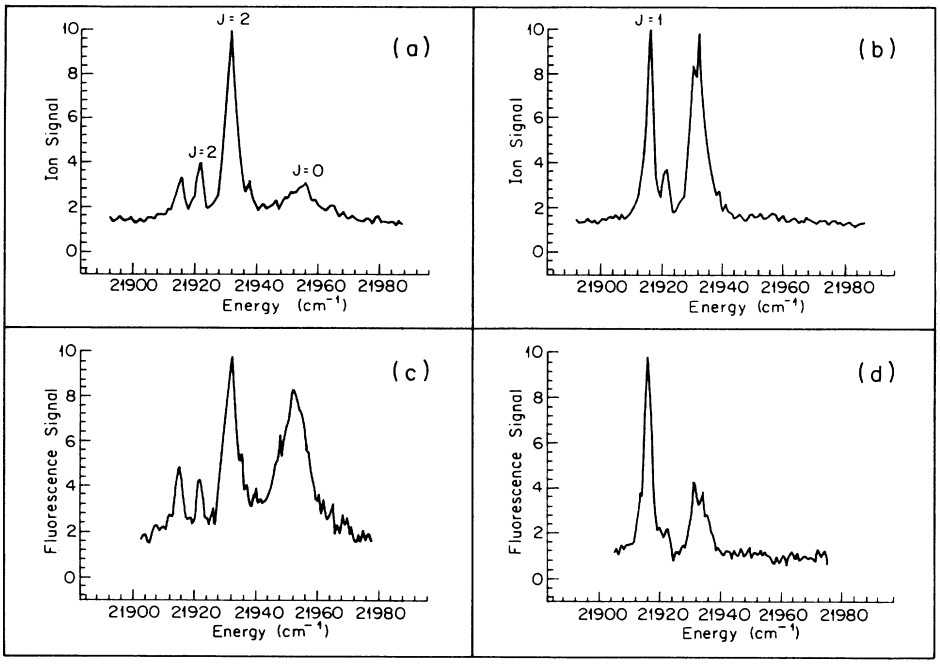

FIG. 3. Total ion [(a) and (b)] and excited ion [(c) and (d)] yield from exciting the $6p_{3/2}15p$ state of barium. (a) and (c) were taken with parallel laser polarizations; (b) and (d) were taken with crossed laser polarizations.

state. It was not possible, even using these four parameters, to fit the four splittings exactly; however, the error for any particular resonance was less than half a linewidth. Our reported values were obtained by using a weighted least-squares-minimization procedure that produced energies and the *LS* composition of the wave functions by diagonalizing the interaction matrix. The resonances were weighted equally, except for the wide $J=0$ state, which was weighted by half as much due to its large linewidth. Table I summarizes the fitted electron interactions for the $6p_{3/2}15p$ states.

Also in Table I, we have listed our calculated values for the two-electron interactions, where we have evaluated the integrals in Eqs. (1) and (2). We used wave functions that were constructed using an exponential core charge distribution for the Ba^{2+} hard core. The core radius was chosen to give the correct quantum defect for the $Ba^{+}(6p)$ wave function. The *np* Rydberg wave function was then created using the same core potential, the shielding from the $6p$ wave function and a Lagrange multiplier to force orthogonality on the two *p* wave functions. The exchange integrals were particularly sensitive to the orthogonalization procedure. Nevertheless, there is good agreement between the fitted and calculated parameters.

The excitation strengths and the coupling strength to the $6p_{1/2}\epsilon p$ continuum serve as additional checks on the validity of the fitting procedure. Under the assumption that the $6snp$ initial state is well described as a $^1P_1$ pure state, then the excitation strength to each state in the multiplet is proportional to its admixture of $^1S_0$, $^1P_1$, or $^1D_2$ character. Moreover, for parallel polarized lasers the ratio of $^1S_0$ excitation to $^1D_2$ excitation should be 1:2. For perpendicularly polarized lasers, the ratio of $^1P_1$ ex-

TABLE II. Excitation strengths of the $6p_{3/2}15p$ multiplet as measured from the spectra and as calculated from the fitted values of the electron interactions given in Table I. Parallel and perpendicular refer to the relative polarization of the two excitation lasers. The transition rates were normalized to that of the $J=0$ state.

	Measured		Calculated	
J	Parallel	Perpendicular	Parallel	Perpendicular
0	1	<0.1	1	0
1	<0.1	0.9±0.1	0	1
1			0	0.3
2	1.5±0.1	1.1±0.1	1.6	1.2
2	0.2±0.02	0.1±0.02	0.02	0.02

TABLE III. Measured linewidths and branching ratios of the $6p_{3/2}15p$ multiplet. The measured partial widths are derived from the linewidths and the branching ratios; the calculated partial linewidths are calculated using the fitted values of the two-electron interactions given in Table I. All linewidths are in units of cm^{-1}.

J	Linewidth	Fluorescence Ratio	Partial width Measured	Calculated
0	15.0±2.0	0.97±0.03	15±2	16
1	2.3±0.5	0.67±0.05	1.5±0.3	1.3
2	5.0±0.5	0.28±0.03	1.4±0.2	1.7
2	1.6±0.5	0.3±0.1	0.5±0.2	0.1

citation to $^1D_2$ excitation should be 1:1, with the $^1D_2$ excitation decreasing by a factor of $\frac{3}{4}$ relative to the parallel polarized case. Table II lists our observed excitation strengths and those calculated from the wave functions produced by diagonalizing the interaction matrix. The agreement is good, except for the smaller $J=2$ state, which has an amplitude significantly greater than the nearly zero value predicted from the LS composition of the wave functions. This could either represent larger singlet character in the final state or some admixture of triplet state into the initial state.

The fluorescence spectra of Fig. 3 show the relative branching ratio for autoionization into the $6p_{1/2}\epsilon l$ continuua (where $l=1$ or 3) as compared to the total ionization into all available final ionic states. For the $J=0$ state, only the $6p_{1/2}\epsilon p$ continuum is possible, and this path seems to dominate all others. The $6p_{1/2}15p$, $J=0$ state, which has all the same continuua available, except for the $6p_{1/2}\epsilon p$, has an autoionization width that is smaller than the $6p_{3/2}15p$, $J=0$ by well over a factor of 30. (It appeared no larger than our laser linewidth, even for $n=15$.) Consequently, we have used the $6p_{3/2}np$, $J=0$ state to put an absolute scale on the relative branching ratios obtained from Fig. 3. From the branching ratio, and the observed linewidth of each state, which determines its total autoionization rate, we can obtain the partial width due to autoionization into the excited ion continuua. In Table III, we compare these partial autoionization rates with those calculated from the two-electron interactions produced by fitting the spectra. The agreement is excellent.

CONCLUSION

The $6p_{3/2}np$ states of barium have been shown to form multiplets that are well described by a single configuration. The two-electron interactions and the one-electron fine-structure interactions account well for the splittings among the multiplet, the LS composition of the states, and the autoionization of each of the states into the $6p_{1/2}+\epsilon p$ continuum. A simple two-electron calculation, which uses a model for the Ba^{2+} hard core, produces good agreement with the measured values. This suggests that simple approximations of such interactions are often sufficient, when a detailed description of the states is not necessary.

The interactions described here do lead to configuration mixing, in the form of autoionization from the excited fine-structure state ($6p_{3/2}$) to the lower fine-structure state's continuum ($6p_{1/2}$). As has been seen in the $6p_{3/2}ns$ states of barium, the mechanism for this autoionization is primarily the quadrupole interaction. It should be expected that this will also be the dominant interchannel interaction, which will couple $6p_{1/2}np$ states to $6p_{3/2}n'p$ states for values of $n'<12$. Work is in progress to examine this prediction.

ACKNOWLEDGMENTS

This work was supported by the National Science Foundation under Grant No. PHY8500885.

[1]See, for example, J. A. Armstrong, P. Esherick, and J. J. Wynne, Phys. Rev. A **15**, 180 (1977); R. Beigang and D. Schmidt, Phys. Scr. **27**, 172 (1983); J. R. Rubbmark, S. A. Borgstrom, and K. Bockasten, J. Phys. B **10**, 421 (1977); W. Liang-guo and R. D. Knight, Phys. Rev. A **34**, 3902 (1986).
[2]K. T. Lu and U. Fano, Phys. Rev. A **2**, 81 (1970).
[3]M. J. Seaton, Rep. Prog. Phys. **46**, 167 (1983).
[4]M. Aymar, J. Opt. Soc. Am. B **1**, 239 (1984).
[5]N. H. Tran, P. Pillet, R. Kachru, and T. F. Gallagher, Phys. Rev. A **29**, 2640 (1984).
[6]S. A. Bhatti and W. E. Cooke, Phys. Rev. A **28**, 756 (1983).
[7]E. U. Condon and G. H. Shortley, *The Theory of Atomic Spectra* (Cambridge University Press, Cambridge, 1970).
[8]W. E. Cooke and C. L. Cromer, Phys. Rev. A **32**, 2725 (1985).
[9]J. A. Armstrong, J. J. Wynne, and P. Esherick, J. Opt. Soc. Am. **69**, 211 (1979).
[10]W. E. Cooke, S. A. Bhatti, and C. L. Cromer, Opt. Lett. **7**, 69 (1982).